IEEE Access
Multidisciplinary | Rapid Review | Open Access Journal

Received May 27, 2021, accepted June 3, 2021, date of publication June 8, 2021, date of current version June 17, 2021.

Digital Object Identifier 10.1109/ACCESS.2021.3087626

Optimal Power Flow Problem Solution Through a Matheuristic Approach

JUAN M. HOME-ORTIZ, WMERSON CLARO DE OLIVEIRA, AND JOSÉ ROBERTO SANCHES MANTOVANI, (Member, IEEE)
Department of Electrical Engineering, Sao Paulo State University, Ilha Solteira 15385000, Brazil

Corresponding author: Juan M. Home-Ortiz (juanmanuelhome@gmail.com)

This work was supported in part by the São Paulo Research Foundation (FAPESP) under Grant 2019/01841-5, Grant 2019/23755-3, and Grant 2015/21972-6; in part by the Coordination for the Improvement of Higher Education Personnel (CAPES) under Grant 001; and in part by the Brazilian National Council for Scientific and Technological Development (CNPq) under Grant 164751/2018-1 and Grant 304726/2020-6.

ABSTRACT The optimal power flow (OPF) problem is a widely studied subject in the literature that has been solved through classical and metaheuristic optimization techniques. Nowadays, significant advances in computational resources and commercial optimization solvers allow solving complex optimization problems by combining the best of both worlds in approaches that are known as matheuristics, however, in order to solve the OPF problem, matheuristic approaches have been little explored. In this regard, this paper presents a novel Variable Neighborhood Descent (VND) matheuristic approach to solve the OPF problem for large-scale systems. The proposed algorithm combines the classic OPF model and the VND heuristic algorithm. The OPF problem is formulated as a mixed-integer nonlinear programming (MINLP) model, in which the objective function aims to minimize the fuel generation costs, subject to the physical and operational constraints of the power system. The integer variables of this MINLP model represent the control of taps positions of the on-load tap changers and the reactive shunt compensation equipment. To validate the proposed methodology, 17 power systems of specialized literature were tested with sizes from 14 to 4661 buses, and the obtained solutions are compared with the solutions provided by the commercial optimization solver Knitro. Results show the superiority of the proposed matheuristic algorithm compared with Knitro to solve the MINLP-OPF model for large-scale systems.

INDEX TERMS Matheuristic optimization, mixed-integer nonlinear programming, optimal power flow, variable neighborhood search.

NOMENCLATURE

Sets and Indexes:

Γ_B	Set of buses
Γ_{CB}	Set of buses with controllable capacitive reactive power (capacitor bank)
Γ_G	Set of generation buses
Γ_L	Set of transmission lines
Γ_T	Set of lines with an OLTC
i	Index of buses
ij	Index of lines

Parameters:

$\hat{n}_{ij}^{t}$	Current position of the tap of the OLTC at line ij
$\hat{n}_{i}^{s}$	Current position of the shunt compensator at bus i
ρ	Penalty parameter
θ_{ij}^{max}	Maximum voltage angle drop
θ_{ij}^{min}	Minimum voltage angle drop
a_i, b_i, c_i	Active power production cost coefficients of generation unit i
b_{ij}^{sh}	Shunt susceptance of line ij
g_i^{sh}, b_i^{sh}	Shunt conductance and susceptance at node i
g_{ij}, b_{ij}	Series conductance and susceptance of line ij
k^t, k^s	Maximum number of tap change of OLTC and shunt compensators
$n_{ij}^{t,max}$	Maximum number of tap positions of the OLTC at line ij
$n_i^{s,max}$	Maximum number of shunt compensator modules at node i

The associate editor coordinating the review of this manuscript and approving it for publication was Nagesh Prabhu.

P_{D_i} Active power demand of node i
$P_{G_i}^{max}$ Maximum active power generation capacity of generation unit i
$P_{G_i}^{min}$ Minimum active power generation capacity of generation unit i
Q_{D_i} Reactive power demand of node i
$Q_{G_i}^{max}$ Maximum reactive power generation capacity of generation unit i
$Q_{G_i}^{min}$ Minimum reactive power generation capacity of generation unit i
r_{ij} Maximum voltage regulation ratio of the OLTC at line ij
S_{ij}^{max} Maximum apparent power flow of line ij
v_i^{max} Maximum voltage magnitude of node i
v_i^{min} Minimum voltage magnitude of node i

Discrete Variables:

n_i^s Position of the reactive control of the shunt compensator at node i
n_{ij}^t Tap position of the OLTC at line ij

Continuous Variables:

θ_{ij} Voltage angle difference
$\tilde{P}_{G_i}$ Slack variable for active power at node i
$\tilde{Q}_{G_i}^c$ Slack variable for capacitive reactive power at node i
$\tilde{Q}_{G_i}^i$ Slack variable for inductive reactive power at node i
a_{ij} Transformation ratio of the OLTC installed at line ij
P_{G_i} Active power generated by the generation unit at node i
p_{ij}^+, p_{ij}^- Active power flows of line ij
Q_{G_i} Reactive power generated by the generation unit at node i
q_{ij}^+, q_{ij}^- Reactive power flows of line ij
v_i Voltage magnitude at node i
w_i Auxiliary variable that determines the percentage capacity of the shunt compensator installed at bus i (value between 0 and 1)

I. INTRODUCTION

The electric power systems (EPS) must supply energy to the consumers with quality, safety, and economy. Therefore, the EPS must operate with safely and good performance, through the appropriate adjustment of control variables, to supply energy at minimum cost and maximum profit. The most common way to determine an economic static operating state of the EPS is by solving the optimal power flow (OPF) problem, which is a computational simulation tool, essential in solving problems in the planning and operation of EPS. It includes a set of optimization problems that aim to obtain the adjustments of the control variables, for the operating states of the EPS (dispatch of active and reactive powers, reduction of operating costs, voltage stability criteria, among others), addressing a set of physical and operational constraints for different devices and the transmission network. The OPF problem addresses the optimization of the EPS operational state [1]. The control variables that are determined by the solution of the OPF problem define an operating state to attend the power load while the physical and operational limits of the system are satisfied [2].

A. LITERATURE REVIEW

In the literature can be found several optimization models for the OPF problem, adopting different modeling approaches, single- and multi-objective views, constraints, and decision variables [3]–[8]. In this regard, several solution techniques for the OPF problem have been proposed, among which stand out are mixed-integer programming (MIP) models, convex models, specialized mathematical algorithms, methods based on heuristics, and metaheuristics.

In [9], a distributed nonlinear control-based algorithm is used to determine the optimal power dispatch in power systems considering the control of reactive power generation. In [10], a nonlinear programming (NLP) model is proposed for the OPF problem, the optimization model is represented in rectangular coordinates, and a primal-dual interior-point method (IPM) is used to solve it. The objective function is to minimize the loss of active power in the transmission system, considering the physical and operational constraints of the network. The tests were performed on systems known from the literature such as IEEE- 30, 57, 118, and 300 bus systems. The results obtained allow us to conclude that the IPM can efficiently solve the nonlinear OPF problem, and that computational performance is equally efficient, both in the space of the rectangular and polar variables. In [11], the OPF problem is solved via successive linear approximations of the power flow equations using the polar formulation of the problem. The development of convex models have been addressed in [12]–[16], however, in many cases, these approaches consider several approximations and the global optimal solution for the problem cannot be reached, also, the integrality of the control variables is not addressed in these works.

Metaheuristic techniques have a large background in solving the OPF problem, in this regard, some examples of metaheuristic techniques that have been used are Simulated Annealing in [17], [18], Tabu Search [19], Genetic Algorithms [2], [20], Evolutionary Programming [21] Particle Swarm Optimization (PSO) [22], Differential Evolution (DE) Algorithm [23], Cuckoo search algorithm [24], Teaching-Learning-based optimization algorithm [25], League Championship algorithm [26], black-hole-based optimization approach [27], monarch butterfly optimization [28], and Gravitational search algorithm [29]. Hybrid metaheuristic approaches can also be found in the literature. In [30], the authors propose a Hybridized Algorithm with DE algorithm and Invasive Weed Optimization (IWO) to handle both continuous and discrete control variables of the OPF problem.

In [31] a hybrid Enhanced Genetic Algorithm (EGA) with an incremental power flow model was proposed. A hybrid EGA with a boundary method to handle higher and lower violations was proposed in [32]. In [33], a Simulated Annealing algorithm was hybridized with a PSO algorithm to solve the OPF problem. One of the main advantages of metaheuristic optimization includes its capability of handling the nonlinearities that characterize a realistic formulation as well as non-continuous variables in an efficient manner, without linearization of the OPF formulation. Moreover, metaheuristic algorithms can be applied so solve the OPF problem with multi-objective approaches such as environmental objectives immune algorithm [34], PSO [35], and Flower Pollination Algorithm [36].

Recent works have used new metaheuristics techniques to solve the OPF problem considering different objective functions, tap control of the on-load tap changers (OLTC), and shunt compensation control [30], [37]–[42]. In [30], a hybrid DE and IWO algorithm minimizes the fuel cost and real power losses considering tap control of the OLTCs and shun compensation control. In [37] a moth swarm algorithm is used to solve the problem, the formulation also considers the optimization of the tap charger ratios and shunt compensator. A similar OPF problem considering tap control of OLTCs and shunt compensators is solved in [43] through a grey wolf optimizer algorithm. In [38], a modified grasshopper optimization algorithm is proposed to solve the OPF problem considering single and multi-objective functions. In [39], a modified Sine-Cosine algorithm with Levy flight is proposed to solve the OPF problem. In [40], an optimization algorithm based on metaheuristic Colliding Bodies Optimization (CBO) is proposed to solve the OPF problem. This metaheuristic is inspired by nature, based on the law of collision between two bodies. To validate the methodology, an algorithm based on the Social Spider Optimization (SSO) metaheuristic is used in [41] to solve the OPF problem, this SSO algorithm is based on simulation of cooperative behavior of social-spiders. In the formulation, several objectives are considered independently, namely: generation cost, losses of active power, emission of polluting gases, voltage deviation, and an index of voltage stability. In [42] a hybrid algorithm is presented that combines Differential Evolution and Harmony Search to solve the OPF problem. The objective function of the model contemplates the generation costs, losses of active power in transmission lines, and voltage stability index. The constraints are active and reactive power balance, prohibited operating zones, and valve point loading effects of generators. In the formulation, discrete controls of the taps of the OLTCs and reactive power compensation equipment are also considered. In the above works, the most common systems are IEEE30, IEEE57, and IEEE118, while large-scale power systems are not considered to validate the algorithms.

B. RESEARCH GAP AND NOVEL CONTRIBUTIONS

Matheuristic optimization techniques are approaches that combine metaheuristic algorithms with mathematical optimization models to solve complex optimization problems, however, these techniques have not gotten much attention when it comes to solving power systems optimization problems. Thus, motivated by the above literature review, where there is not any matheuristic approach to solve the OPF problem, in this work, it is proposed a novel algorithm based on a matheuristic optimization methodology to solve it.

In this paper, the OPF problem is formulated as a mixed-integer nonlinear-programming (MINLP) model where the integer variables determine the OLTCs' tap positions and the shunt reactive compensators operation. Commercial optimization solvers can be used to find local optimal solutions of this model in small- medium-scale power systems, however they fail to solve the problem in large-scale power systems. To tackle this issue, it is proposed an innovative matheuristic algorithm (MA) that comprises the MINLP-OPF model and the Variable Neighborhood Descent (VND) heuristic method.

According to the presented state of the art, the contributions of this paper are the follows:

1) Proposing a new VND-matheuristic algorithm (VND-MA) to solve the OPF problem in large-scale power systems. In this approach, the MINLP-OPF model is decomposed into a subproblem with real variables that are solved using nonlinear programming techniques and another subproblem that controls the discrete variables of the MINLP-OPF model using the variable neighborhood heuristic method.
2) Proposing a new set of neighborhood structures for the OPF problem that are based on the optimization of NLP models. These structures are a novel view for the optimization of power systems that can be applied to other problems of electrical power system planning.
3) The approach is able to solve with precision and reliability the OPF problem for large-scale power systems with thousands of buses on an adequate computational time to solve the OPF problem for planning the operation of electrical power systems.

The remainder of this paper is organized as follows: Section II presents the MINLP formulation of the OPF problem. Section III presents the proposed matheuristic approach that uses the MINLP model for the OPF problem and a VND metaheuristic algorithm to determine the optimal value of the decision variables of the problem. Section IV and V, respectively, present the results and discussions of the simulations. Finally, relevant conclusions are drawn in Section VI.

II. MATHEMATICAL MODEL

The OPF model considered in this work is an MINLP model in which the objective function represents the minimization of the generation costs, subject to a set of physical and operational constraints of the power system. The control variables of the problem are the tap position of the OLTCs and the position of the shunt compensators. On the other hand, the state variables are the active and reactive power injected by generating units, the voltage magnitude at nodes, voltage

phase at nodes, and power flow through the transmission lines. The OPF problem is formulated in (1)-(17) [4].

$$\min f(P_{G_i}) = \sum_{i\in\Gamma_G} a_i P_{G_i}^2 + b_i P_{G_i} + c_i. \quad (1)$$

subject to

$$P_{G_i} - g_i^{sh} v_i^2 - \sum_{ij\in\Gamma_L} p_{ij}^- - \sum_{ij\in\Gamma_L} p_{ji}^+ = P_{D_i}, \quad (2)$$

$$Q_{G_i} - b_i^{sh} v_i^2 w_i - \sum_{ij\in\Gamma_L} q_{ij}^- - \sum_{ij\in\Gamma_L} q_{ji}^+ = Q_{D_i}, \quad (3)$$

$\forall (i \in \Gamma_B)$

$$p_{ji}^- = (a_{ij}v_i)^2 g_{ij} - (a_{ij}v_i)v_j(g_{ij}cos(\theta_{ij})) + b_{ij}sen(\theta_{ij})), \quad (4)$$

$$p_{ji}^+ = v_j^2 g_{ij} - (a_{ij}v_i)v_j(g_{ij}cos(\theta_{ij})) - b_{ij}sen(\theta_{ij})), \quad (5)$$

$$q_{ji}^- = -(a_{ij}v_i)^2 \left(b_{ij} + \frac{b_{ij}^{sh}}{2}\right) + (a_{ij}v_i)v_j(b_{ij}cos(\theta_{ij})) - g_{ij}sen(\theta_{ij})), \quad (6)$$

$$q_{ji}^+ = -v_i^2 \left(b_{ij} + \frac{b_{ij}^{sh}}{2}\right) + (a_{ij}v_i)v_j(b_{ij}cos(\theta_{ij})) + g_{ij}sen(\theta_{ij})), \quad (7)$$

$\forall (ij \in \Gamma_L)$

$$w_i = \left(\frac{n_i^s}{n_i^{s,max}}\right) \quad \forall (i \in \Gamma_{CB}), \quad (8)$$

$$a_{ij} = 1 + \left(\frac{n_{ij}^t r_{ij}}{n_{ij}^{t,max}}\right) \quad \forall (ij \in \Gamma_T), \quad (9)$$

$$v_i^{min} \le v_i \le v_i^{max} \quad \forall (i \in \Gamma_B), \quad (10)$$

$$P_{G_i}^{min} \le P_{G_i} \le P_{G_i}^{max} \quad \forall (i \in \Gamma_G), \quad (11)$$

$$Q_{G_i}^{min} \le Q_{G_i} \le Q_{G_i}^{max} \quad \forall (i \in \Gamma_G), \quad (12)$$

$$(p_{ij}^-)^2 + (q_{ij}^-)^2 \le S_{ij}^{max} \quad \forall (ij \in \Gamma_L), \quad (13)$$

$$(p_{ij}^+)^2 + (q_{ij}^+)^2 \le S_{ij}^{max} \quad \forall (ij \in \Gamma_L), \quad (14)$$

$$\theta_{ij}^{min} \le \theta_{ij} \le \theta_{ij}^{max} \quad \forall (i \in \Gamma_L), \quad (15)$$

$$0 \le n_i^s \le n_i^{s,max} \quad \forall (i \in \Gamma_{CB}), \quad (16)$$

$$0 \le n_{ij}^t \le n_{ij}^{t,max} \quad \forall (i \in \Gamma_T). \quad (17)$$

$$n_i^s, n_{ij}^t \in \mathbb{Z}$$

The objective function $f(P_{G_i})$ shown (1), minimizes the total fuel cost of the power generation units according to the active power generated using its positive costs coefficients a_i, b_i, and c_i, which are the most used in the literature.

Equations (2) and (3) represent the active and reactive power balance of the system. Equations (4)-(7) determine the active and reactive power flow through lines ij using the polar format which is one of the most accurate ways to represent the power flow in transmission systems [10], [44], [45]. Equation (8) determine the percentages of reactive power injection capacity of the shunt compensators where the integer variable n_i^s determines the number of the operating shunt compensators at the bus i. For the OLTC installed at line ij, equation (9) determines the voltage transformation ratio a_{ij}, where the integer variable n_{ij}^t determines the tap position, and parameter r_{ij} defines the maximum voltage regulation ratio. Constraint (10) represents the operational limits of the magnitude of voltage on the system. Constraints (11) and (12) represent the active and reactive power generation, respectively. The quadratic constraints (13) and (14) model the thermal limit of the transmission lines. Constraint (15) represents the limits of the voltage angular drop between the buses. Constraint (16) represents the range operating limit of the shunt compensators, while constraint (17) specifies the range operating limit of the OLTCs' taps.

Modern optimization solvers for MINLP problems can be used to solve the OPF model (1)-(17) in small- and medium-scale systems, however, for large-scale systems, this strategy can lead to high computational times or convergence issues. In this way, this paper proposes a matheuristic approach that combines the functionalities of the VND heuristic algorithm and nonlinear programming models to solve the MINLP-OPF model (1)-(17). This technique can handle the nonlinearities and non-convexity that characterize this problem, discrete and continuous variables, as well as all the constraints in an efficient way.

III. SOLUTION TECHNIQUE

This section presents the optimization concepts used to develop the proposed matheuristic algorithm. Besides, fundamentals of the VND heuristic algorithm and its adaptation to solve the OPF problem are presented.

A. MATHEURISTIC OPTIMIZATION TECHNIQUES

The matheuristic optimization techniques are algorithms that combine heuristics and well-defined mathematical models to solve complex optimization problems. An important aspect of these algorithms is that they explore the characteristics of the mathematical model of the problem under analysis [46]. In general, matheuristic optimization techniques aim to take advantage of the optimality of the exact mathematical solution method and the efficiency of a metaheuristic algorithm.

In this paper, the proposed matheuristic algorithm (MA) to solve the OPF model (1)-(17) is composed of a Variable Neighborhood Search (VNS) heuristic algorithm and NLP models derived from the MINLP model (1)-(17). In this approach, the exploration of the neighborhood structures is performed using the solution of these NLP models, in this regard, there is an implicit decomposition of the problem where the VNS algorithm operates at a higher level coordinating the interaction between neighborhood structures and controlling the executions of the NLP subproblems that are at the lower level. This strategy allows for obtaining an optimal globally or a local solution for each neighborhood structure.

B. VARIABLE NEIGHBORHOOD SEARCH

The VNS is a heuristic optimization technique based on local search, where the space of solutions is explored through systematic changes in the neighborhood structures [47]. The philosophy of the VNS algorithm is based on diversifying the search process, alternating the neighborhood whenever a certain neighborhood stops evolving towards

quality solutions. The algorithm explores the neighborhood search space of the current solution gradually and intensifies the search in the region of the domain of the problem for a new solution, only executing explorations in this region to generate better solutions.

The VND is the most simplified version of the VNS algorithms. In a general way, the VND heuristic algorithm consists of a deterministic process, which starts from an initial solution x and finds a more pronounced descent direction from it, within a neighborhood $N(x)$. In this way, it moves along the direction of maximum decrease of the objective function $f(x)$, and if there is no direction of descent, then the heuristic is interrupted, and another neighboring structure is explored [47].

C. VND DEDICATED TO OPF SOLUTION

The proposed MA to solve the MINLP-OPF model (1)-(17) consists of the VND heuristic philosophy together with the solution of NLP models via commercial solvers. The proposed approach consists of the following steps:

1) Representation of a solution for the discrete variables.
2) Modified OPF model.
3) Initial solution.
4) Neighborhood structures.
5) Stopping criterion.

1) REPRESENTATION OF A SOLUTION FOR THE DISCRETE VARIABLES

According to (18) and (19), the discrete variables of the problem are represented by two vectors, n^t and n^s, for taps of the OLTCs and shunt compensators, respectively.

$$n^t = (n^t_{ij}, \ldots, n_l) \quad \forall (ij \in \Gamma_T), \tag{18}$$

$$n^s = (n^s_i, \ldots, n_b) \quad \forall (i \in \Gamma_{CB}). \tag{19}$$

The vector n^t, has dimension l, where l is the number of lines of the system that have an OLTC. The vector n^s has dimension b, where b corresponds to the number of a bus with shunt compensation. In this paper, the tap positions of the OLTCs must belong to the discrete set $n^t_{ij} \in \{-16, -15, \ldots, 0, \ldots, 15, 16\}$ and, the variables that represent the control switches of the reactive shunt compensators belong to the set $n^s_i \in \{0, 1, 2, 3, 4\}$, that correspond to the discrete percentage values (0, 25, 50, 75, and 100)% of reactive power being injected into the system bus.

2) MODIFIED OPF MODEL

One of the characteristics of metaheuristic optimization techniques is allowing infeasible solutions to improve the exploration of the search space. Thus, minor changes to the OPF model formulation (1)-(17) are necessary.

To avoid an infeasible solution due to a lack of power generation, an additional power generation is considered at each node of the system. In this regard, the slack variables $\tilde{P}_{G_i}$, $\tilde{Q}^c_{G_i}$, and $\tilde{Q}^i_{G_i}$ are included in the power flow balance formulation. The modified power balance constraints are presented in (20) and (21).

$$P_{G_i} + \tilde{P}_{G_i} - g^{sh}_i v^2_i - \sum_{ij \in \Gamma_L} p^-_{ij} - \sum_{ij \in \Gamma_L} p^+_{ji} = P_{D_i}, \tag{20}$$

$$Q_{G_i} + \tilde{Q}^c_{G_i} - \tilde{Q}^i_{G_i} - b^{sh}_i v^2_i w_i - \sum_{ij \in \Gamma_L} q^-_{ij} - \sum_{ij \in \Gamma_L} q^+_{ji} = Q_{D_i}, \tag{21}$$

$$\tilde{P}_{G_i}, \tilde{Q}^c_{G_i}, \tilde{Q}^i_{G_i} \geq 0.$$
$$\forall (i \in \Gamma_B)$$

These slack variables must be penalized in the objective function of the problem according to (22).

$$f^{PN} = \rho \sum_{i \in \Gamma_B} \left((\tilde{P}_{G_i})^2 + (\tilde{Q}_{G_i})^2 + (\tilde{Q}_{G_i})^2 \right). \tag{22}$$

Finally, the modified MINLP OPF model is presented in the following formulation:

$$\begin{aligned} &\min F = f(P_{G_i}) + f^{PN} \\ &\text{Subject to :} \\ &\qquad (4) - (17), (20), (21). \end{aligned} \tag{23}$$

The objective function F, shown in (23), simultaneously minimizes the total fuel cost of the power generation units and the penalty function f^{PN}. Note that, for feasible solutions, the slack variables $\tilde{P}_{G_i}$, $\tilde{Q}^c_{G_i}$, and $\tilde{Q}^i_{G_i}$ are equal to zero, thus in the feasible search space, this formulation is equivalent to the original formulation (1)-(17).

3) INITIAL SOLUTION

The initial solution for the algorithm is obtained by solving a relaxed OPF problem, i.e., solving the formulation (1)-(17) considering all the integer variables (n^t_{ij} and n^s_i) as continuous variables. Then, the obtained relaxed solution is rounded to the nearest discrete value determining the vectors n^t and n^s. Knowing the values for the integer variables, the objective function value F is calculated by the solution of the modified OPF model (4)-(17), (20)-(23). The obtained integer solution could be unfeasible from the point of view of the original FPO problem (1)-(17), however, in the modified model the slack variables $\tilde{P}_{G_i}$, $\tilde{Q}^c_{G_i}$, and $\tilde{Q}^i_{G_i}$ guarantee that the problem is always feasible. It is worth mentioning that, if the solution of the relaxed model (1)-(17) leads to an infeasible solution, then the MINLP has no integer solution.

4) NEIGHBORHOOD STRUCTURES

The neighborhood structures aim to determine the better-quality neighbor solution around the current solution of the algorithm. In this work, the neighborhood structures are NLP models obtained from the modified MINLP OPF model (4)-(17), (20)-(23).

All the proposed neighborhood structures in this work have the scheme presented in Fig. 1, where $\hat{n}^t_{ij}$ and $\hat{n}^s_i$ are input parameters that determine the current tap position of the OLTC at line ij and the current position of the shunt compensator at bus i. The first step of each neighborhood

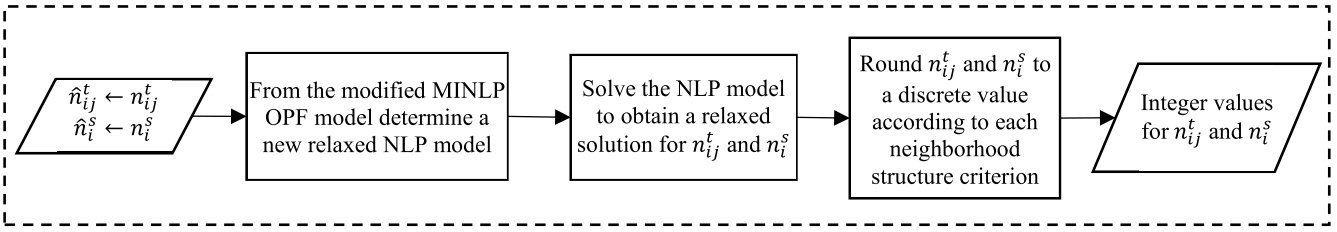

FIGURE 1. Proposed neighborhood structure scheme.

structures is setting the integer parameters $\hat{n}^t_{ij}$ and $\hat{n}^s_i$ at the current values of n^t_{ij} and n^s_i, respectively. Afterward, considering the current solution of the algorithm and the modified MINLP OPF model (4)-(17) and (20)-(23), relax the integrality constraint of all the integer variables of the problem and define a NLP model. Details of the NLP models are presented later as neighborhood structures N_1, N_2 and N_3. Then, for each neighborhood structure, the solution of its corresponding NLP model provides a relaxed value for the variables n^t_{ij} and n^s_i. Afterward, these relaxed solutions are rounded to a discrete value according to a specific criterion. Finally, the output of each neighborhood structure are integer values for variables n^t_{ij} and n^s_i.

Similar to section III-C3, the integer solutions obtained with each neighborhood structure are fixed into the modified OPF model (4)-(17) and (20)-(23) to calculate the objective function value F.

Three neighborhood structures are proposed in this paper and they are described in detail as follows:

a: NEIGHBORHOOD STRUCTURE N_1 - INCREASE/DECREASE THE TAP POSITIONS OF ALL THE OLTCS AND SHUNT COMPENSATORS SIMULTANEOUSLY

The neighborhood structure N_1 allows increasing or decrease the current tap position of all the OLTCs and the position of all the shunt compensators. In this structure, an NLP model is obtained by relaxing the integrality of the integer variables of the problem and including the constraints (24) and (25) into the modified OPF model.

$$\hat{n}^t_{ij} - k^t_{ij} \le n^t_{ij} \le \hat{n}^t_{ij} - k^t_{ij} \quad \forall (ij \in \Gamma_T), \tag{24}$$

$$\hat{n}^s_i - k^s_i \le n^s_i \le \hat{n}^s_i - k^s_i \quad \forall (ij \in \Gamma_{CB}). \tag{25}$$

Constraint (24) allows the tap change of the OLTC at line ij up to $\pm k^t_{ij}$ steps, while constraint (25) allows the modification of the shunt compensator at bus i up to $\pm k^s_i$ steps.

b: NEIGHBORHOOD STRUCTURE N_2 - INCREASE THE TAP POSITION OF THE OLTCS AND SHUNT COMPENSATORS

In the neighborhood structure N_2, the integer variables of the problem are relaxed and the constraints (26)-(29) are included into the modified OPF model. This neighborhood structure analyzes the entire system allowing to increase the current tap position of a single OLTC and a single shunt compensator up to k^t_{ij} and k^s_i steps, respectively.

$$\hat{n}^t_{ij} \le n^t_{ij} \le \hat{n}^t_{ij} + k^t_{ij} \quad \forall (ij \in \Gamma_T), \tag{26}$$

$$\sum_{ij \in \Gamma_T} \hat{n}^t_{ij} \le \sum_{ij \in \Gamma_T} n^t_{ij} \le \sum_{ij \in \Gamma_T} \hat{n}^t_{ij} + k^t, \tag{27}$$

$$\hat{n}^s_i \le n^s_i \le \hat{n}^s_i + k^s_i \quad \forall (i \in \Gamma_{CB}), \tag{28}$$

$$\sum_{i \in \Gamma_{CB}} \hat{n}^s_i \le \sum_{i \in \Gamma_{CB}} n^s_i \le \sum_{i \in \Gamma_{CB}} \hat{n}^s_i + k^s. \tag{29}$$

Constraints (26) and (27) determine the tap positions of the OLTCs, while constraints (28) and (29) determine the positions of the shunt compensators. Constraint (26) allows increasing the tap position of the OLTC at line ij up to k^t_{ij} steps, while constraint (27) restricts the entire system to increase up to k^t steps the sum of all the tap positions of the OLTCs of the system. Constraint (28) allows increasing the shunt compensator at bus i up to k^s_i steps, while (29) restricts the entire system to increase up to k^s the sum of all the shunt compensators connected to the system. Note that, the solution of this model can increase all the OLTCs' taps and all the shunt compensators simultaneously, then, these solutions are ranked and the n^t_{ij} and n^s_i with the greatest increment are selected to increase their current values.

c: NEIGHBORHOOD STRUCTURE N_3 - REDUCE THE TAP POSITION OF THE OLTCS AND SHUNT COMPENSATORS

In the neighborhood structure N_3, the integer variables n^t_{ij} and n^s_i are relaxed and the constraints (30)-(33) are included into the modified OPF model. This neighborhood structure allows reducing the current tap position of a single OLTC and a single shunt compensator up to k^t_{ij} and k^s_i steps, respectively.

$$\hat{n}^t_{ij} - k^t_{ij} \le n^t_{ij} \le \hat{n}^t_{ij} \quad \forall (ij \in \Gamma_T), \tag{30}$$

$$\sum_{ij \in \Gamma_T} \hat{n}^t_{ij} - k^t \le \sum_{ij \in \Gamma_T} n^t_{ij} \le \sum_{ij \in \Gamma_T} \hat{n}^t_{ij}, \tag{31}$$

$$\hat{n}^s_i - k^s_i \le n^s_i \le \hat{n}^s_i \quad \forall (i \in \Gamma_{CB}), \tag{32}$$

$$\sum_{i \in \Gamma_{CB}} \hat{n}^s_i - k^s \le \sum_{i \in \Gamma_{CB}} n^s_i \le \sum_{i \in \Gamma_{CB}} \hat{n}^s_i. \tag{33}$$

Constraints (30) and (31) determine the tap positions of the OLTCs, while constraints (32) and (33) determine the positions of the shunt compensators. Constraint (30) allows the tap reduction of the OLTC at line ij up to k^t_{ij} steps, while constraint (31) limits the entire system to reduce up to k^t steps the sum of all the tap positions of the OLTCs of the system. Constraint (32) allows the reduction of the shunt compensator at bus i up to k^s_i steps, while (33) restrict the entire system to reduce up to k^s the sum of all the shunt compensators connected to the system. Similarly, to neighborhood structure N_2,

all the n_{ij}^t and n_i^s can reduce their values, then, these solutions are ranked and the n_{ij}^t and n_i^s with the greatest reduction are selected to reduce their current values.

It is worth mentioning that these neighborhood structures do not force updating the taps of the OLTCs and shunt compensators when it is not necessary. In this work, $k_{ij}^t = 2$ and $k_i^s = 1$ were used in all the tests.

5) STOPPING CRITERION

The execution of the algorithm is completed when the search process explores all the neighborhood structures, and no improvement of the incumbent solution is obtained.

D. STRUCTURE OF THE PROPOSED ALGORITHM

The proposed matheuristic structure to solve the MINLP-OPF model is illustrated in the flowchart of Fig. 2, where X, represents the current value of all discrete variables of the problem (OLTC's tap positions and shunt compensators), $F(X)$ represents the value of the objective function for X, Υ represents a candidate solution for the problem (discrete values and objective function), X' represents the neighbor solution of X, m is a counter to determine the neighborhood structure to be analyzed, and M is the number of considered neighborhood structures.

The first step to solve the MINLP-OPF model is to obtain an integer initial solution X using the proposed approach presented in III-C3, afterward, determine the objective function value $F(X)$, set the current solution of the algorithm Υ as $\{X, F(X)\}$, and start the counter m at 1 to analyze the first neighborhood structure.

Considering the current solution of the algorithm Υ, use the neighborhood structure N_m to determine a neighbor integer solution X', with its respective objective function value $F(X')$. If the objective function value of the neighbor solution is better than the objective function of the current solution of the algorithm, then, update the current solution of the algorithm Υ as $\{X', F(X')\}$ and set the counter m at 1 to continue the optimization process with the first neighborhood structure. Otherwise, if the objective function value of the neighbor solution is worse than the objective function of the current solution of the algorithm, then, update the counter m at $m + 1$ to continue the optimization process with the next neighborhood structure. The optimization process ends when the counter m is greater than M indicating that all the neighborhood structures have been explored with no improvements in the current solution of the algorithm.

In order to efficiently explore the search space, the neighborhood structure with the greatest impact on the value of the objective function is analyzed at the beginning of the algorithm, thus, note that the analysis of neighborhood structures follows the following order: N_1, N_2 e N_3. This sequence was determined based on the performance of the numerical experiments.

IV. TESTS AND RESULTS

The robustness, efficiency, and scalability of the proposed VND matheuristic algorithm (VND-MA) were

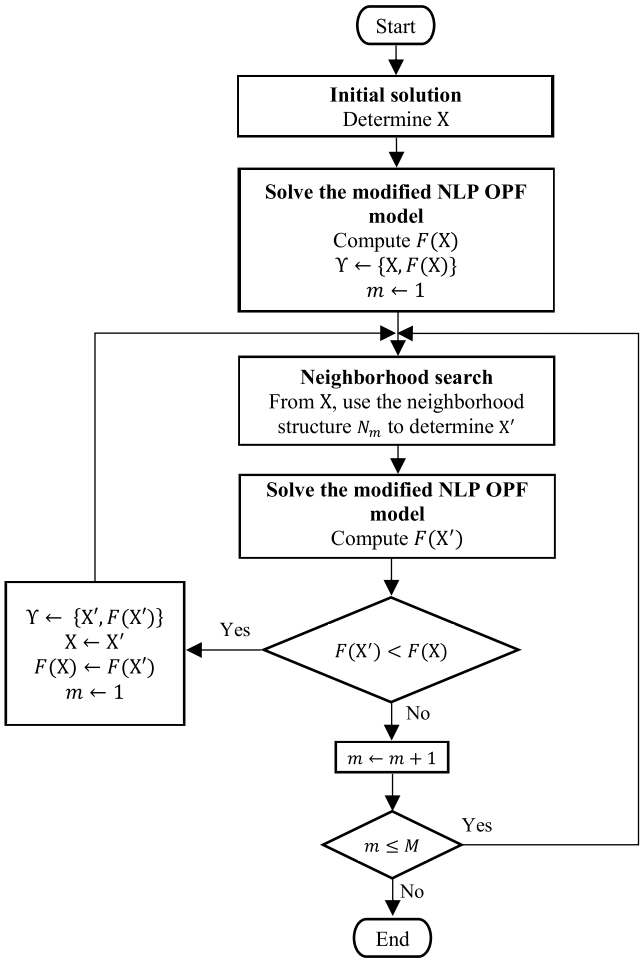

FIGURE 2. Proposed VND matheuristic algorithm.

verified by solving 17 test systems with sizes from 14 to 4661 buses. The test systems simulated in this work are open access data and are available in the PGLib-OPF v19.05 library [48]. Table 1 presents the dimensions of the systems with the names corresponding to the file available in the PGLib-OPF library. Relevant information about the test system *pglib_opf_case89_pegase* can be found in [49]. For all the test systems the OLTCs have the ability to regulate $\pm 10\%$ of input voltage with ± 16 positions for the taps. Furthermore, the solutions obtained by the proposed VND-MA are compared with the three following approaches:

1) The MINLP model (1)-(17) is solved directly using the commercial optimization solver Knitro 12.0.0.
2) Rounding the solution obtained by the optimization of the relaxed model (RR-SOL). This approach equates to the initial solution of the proposed algorithm described in section III-C3. Integer solutions found by this approach are validated in the original FPO model (1)-(17).
3) The OPF model and solution technique of Matpower [50] is used. Note that, this software only considers the dispatch of active power generation, while keeping fixed the variables concerning the taps of the OLTCs and the injections of shunts reactive

TABLE 1. Dimensions of the test systems.

System	Lines with OLTC	Buses with CB	Total of devices
pglib_opf_case14_ieee	3	1	4
pglib_opf_case24_ieee_rts	5	1	6
pglib_opf_case30_ieee	7	2	9
pglib_opf_case39_epri	11	0	11
pglib_opf_case57_ieee	17	3	20
pglib_opf_case89_pegase	50	44	94
pglib_opf_case118_ieee	11	14	25
pglib_opf_case200_tamu	66	4	70
pglib_opf_case300_ieee	129	14	143
pglib_opf_case500_tamu	131	15	146
pglib_opf_case2000_tamu	847	148	995
pglib_opf_case2383wp_k	171	0	171
pglib_opf_case2746wp_k	174	0	174
pglib_opf_case3012wp_k	201	9	210
pglib_opf_case3120sp_k	206	9	215
pglib_opf_case3375wp_k	387	9	396
pglib_opf_case4661_sdet	1329	696	2025

compensators. In this sense, these results are used only as a reference for validating the results obtained with the proposed VND-MA.

The proposed VND-MA algorithm was implemented in the mathematical modeling environment AMPL. Numerical experiments were performed using a DELL XPS with Intel Core TM i7-6700 3.40GHz and 8GB RAM. The knitro option "mip_maxtime_cpu" is used to limit the CPU processing time up to 18000 seconds.

A. PGLIB_OPF_CASE118_IEEE SYSTEM

This subsection presents, for illustrative purposes, the obtained solutions for the pglib_opf_case118_ieee system with the optimization solver Knitro, the proposed rounded strategy RR-SOL, Matpower, and the proposed VND-MA. Table 2 presents the objective function value, and the active and reactive power generation values. Tables 3 and 4 present the tap positions of the OLTCs and the shunt compensators operation, respectively. Finally, the voltage profile for each solution is presented in Fig. 3.

Knitro provides the best solution with an objective function value of 97136.77 $/h, followed by the solution obtained with the proposed VND-MA which is just 0.50 $/h higher. It is worth noting that Table 2 presents the active power injection only for the generation units which have an active power injection greater than zero. In this case, the generation units have similar active power injections for all the obtained solutions including null active power injections in the same generation units. On the other hand, the reactive power injections present different behaviors for all the solutions because the reactive subproblem of the OPF model is strongly non-linear and non-convex.

The positions of the OLTCs' taps determined by Knitro are quite similar to the ones determined by the proposed VND-MA. In these cases, the differences are in the OLTCs at branches 38-37 and 65-66. However, note that these taps positions are close each other. On the other hand, the shunt compensators have different operations in all the solutions.

TABLE 2. Results for the pglib_opf_case118_ieee system.

Variable	Knitro	RR-SOL	Matpower	VND-MA
$f(P_{G_i})$ ($/h)	97136.77	97142.58	97213.61	97137.27
$P_{G_{10}}$ (MW)	505.00	505.00	505.00	505.00
$P_{G_{25}}$ (MW)	70.52	66.42	77.97	67.08
$P_{G_{26}}$ (MW)	485.00	485.00	485.00	485.00
$P_{G_{31}}$ (MW)	17.00	17.00	17.00	17.00
$P_{G_{46}}$ (MW)	20.00	20.00	20.00	20.00
$P_{G_{49}}$ (MW)	223.00	223.00	223.00	223.00
$P_{G_{54}}$ (MW)	53.00	53.00	53.00	53.00
$P_{G_{59}}$ (MW)	308.00	308.00	308.00	308.00
$P_{G_{61}}$ (MW)	195.00	195.00	195.00	195.00
$P_{G_{69}}$ (MW)	840.81	846.32	831.98	845.22
$P_{G_{80}}$ (MW)	509.00	509.00	509.00	509.00
$P_{G_{89}}$ (MW)	467.87	467.02	471.46	467.32
$P_{G_{100}}$ (MW)	653.00	653.00	653.00	653.00
$P_{G_{103}}$ (MW)	31.27	31.39	31.28	31.27
Q_{G_1} (MVAr)	15.00	15.00	15.00	15.00
Q_{G_4} (MVAr)	29.93	27.95	71.07	30.19
Q_{G_6} (MVAr)	36.80	36.72	46.70	36.96
Q_{G_8} (MVAr)	-52.19	-26.01	-4.86	-51.34
$Q_{G_{10}}$ (MVAr)	-84.98	-83.69	-86.33	-84.64
$Q_{G_{12}}$ (MVAr)	43.00	43.00	43.00	43.00
$Q_{G_{15}}$ (MVAr)	30.00	30.00	30.00	30.00
$Q_{G_{18}}$ (MVAr)	44.94	47.79	41.39	46.21
$Q_{G_{19}}$ (MVAr)	24.00	24.00	24.00	24.00
$Q_{G_{24}}$ (MVAr)	18.98	19.48	9.27	19.64
$Q_{G_{25}}$ (MVAr)	101.66	64.95	-47.00	101.85
$Q_{G_{26}}$ (MVAr)	-155.95	-119.91	-6.13	-154.92
$Q_{G_{27}}$ (MVAr)	40.14	40.16	32.10	40.04
$Q_{G_{31}}$ (MVAr)	9.00	9.00	9.00	9.00
$Q_{G_{32}}$ (MVAr)	38.18	38.41	35.84	38.26
$Q_{G_{34}}$ (MVAr)	18.97	15.06	8.56	18.63
$Q_{G_{36}}$ (MVAr)	24.00	23.73	23.64	24.00
$Q_{G_{40}}$ (MVAr)	39.25	38.45	38.72	39.02
$Q_{G_{42}}$ (MVAr)	26.55	27.36	22.30	23.21
$Q_{G_{46}}$ (MVAr)	8.52	10.00	-0.54	2.93
$Q_{G_{49}}$ (MVAr)	-85.00	-84.62	-85.00	-85.00
$Q_{G_{54}}$ (MVAr)	27.00	27.00	27.00	27.00
$Q_{G_{55}}$ (MVAr)	23.00	23.00	23.00	23.00
$Q_{G_{56}}$ (MVAr)	15.00	15.00	15.00	15.00
$Q_{G_{59}}$ (MVAr)	108.25	100.73	108.77	111.62
$Q_{G_{61}}$ (MVAr)	-20.11	-14.92	-11.25	-0.71
$Q_{G_{62}}$ (MVAr)	12.49	12.46	1.50	-11.37
$Q_{G_{65}}$ (MVAr)	137.68	150.66	200.00	160.30
$Q_{G_{66}}$ (MVAr)	-60.15	-56.04	-67.00	-67.00
$Q_{G_{69}}$ (MVAr)	-300.00	-300.00	-256.10	-300.00
$Q_{G_{70}}$ (MVAr)	21.80	30.03	32.00	19.70
$Q_{G_{72}}$ (MVAr)	-3.47	-3.45	-3.04	-3.42
$Q_{G_{73}}$ (MVAr)	-1.41	-1.40	1.33	-1.39
$Q_{G_{74}}$ (MVAr)	9.00	9.00	9.00	9.00
$Q_{G_{76}}$ (MVAr)	23.00	23.00	23.00	23.00
$Q_{G_{77}}$ (MVAr)	70.00	70.00	70.00	70.00
$Q_{G_{80}}$ (MVAr)	31.85	29.49	-28.52	32.84
$Q_{G_{85}}$ (MVAr)	23.00	23.00	23.00	23.00
$Q_{G_{87}}$ (MVAr)	4.99	5.00	5.00	5.00
$Q_{G_{89}}$ (MVAr)	-5.22	1.04	-8.76	-5.02
$Q_{G_{90}}$ (MVAr)	45.87	45.83	45.97	45.86
$Q_{G_{91}}$ (MVAr)	1.69	1.76	1.82	1.68
$Q_{G_{92}}$ (MVAr)	9.00	9.00	9.00	9.00
$Q_{G_{99}}$ (MVAr)	7.11	6.94	7.53	7.07
$Q_{G_{100}}$ (MVAr)	18.57	29.30	8.90	18.73
$Q_{G_{103}}$ (MVAr)	9.83	12.66	9.94	9.82
$Q_{G_{104}}$ (MVAr)	23.00	23.00	23.00	23.00
$Q_{G_{105}}$ (MVAr)	23.00	23.00	23.00	23.00
$Q_{G_{107}}$ (MVAr)	15.39	17.17	12.18	13.82
$Q_{G_{110}}$ (MVAr)	23.00	23.00	23.00	23.00
$Q_{G_{111}}$ (MVAr)	2.91	4.37	2.92	2.91
$Q_{G_{112}}$ (MVAr)	16.24	17.51	16.24	16.24
$Q_{G_{113}}$ (MVAr)	1.33	4.30	-2.80	2.89
$Q_{G_{116}}$ (MVAr)	278.09	275.34	281.95	283.15

TABLE 3. OLTCs of the pglib_opf_case118_ieee system.

Branch	Knitro		RR-SOL		VND-MA		Matpower
	n_{ij}^t	a_{ij}	n_{ij}^t	a_{ij}	n_{ij}^t	a_{ij}	a_{ij}
8- 5	3	1.019	4	1.025	3	1.019	0.985
26- 25	-7	0.956	-5	0.969	-7	0.956	0.960
30- 17	2	1.012	2	1.012	2	1.012	0.960
38- 37	3	1.019	5	1.031	4	1.025	0.935
63- 59	5	1.031	6	1.038	5	1.031	0.960
64- 61	1	1.006	1	1.006	1	1.006	0.985
65- 66	9	1.056	9	1.056	10	1.063	0.935
68- 69	15	1.094	14	1.087	15	1.094	0.935
81- 80	0	1.000	-1	0.994	0	1.000	0.935
86- 87	1	1.006	-3	0.981	1	1.006	1.000
68- 116	-2	0.988	-5	0.969	-2	0.988	1.000

TABLE 4. Shunt compensators of the pglib_opf_case118_ieee system.

Bus	Knitro		RR-SOL		VND-MA		Matpower
	n_i^s	(MVAr)	n_i^s	(MVAr)	n_i^s	(MVAr)	(MVAr)
5	0	0.00	2	-22.47	0	0.00	-44.78
34	4	15.65	3	11.72	3	11.73	15.63
37	0	0.00	1	-7.02	0	0.00	-28.09
44	3	7.53	3	7.47	3	7.46	10.01
45	4	9.86	3	7.32	4	9.75	9.78
46	4	10.15	3	7.55	4	10.00	9.99
48	2	7.62	2	7.59	1	3.77	15.23
74	4	11.94	3	8.84	4	11.90	11.89
79	4	21.01	3	15.50	4	21.00	21.23
82	4	20.93	3	15.48	4	20.93	21.07
83	4	10.56	3	7.81	4	10.55	10.61
105	4	21.34	3	15.95	4	21.34	21.34
107	2	3.16	2	3.16	3	4.74	6.32
110	4	6.21	2	3.09	4	6.21	6.21

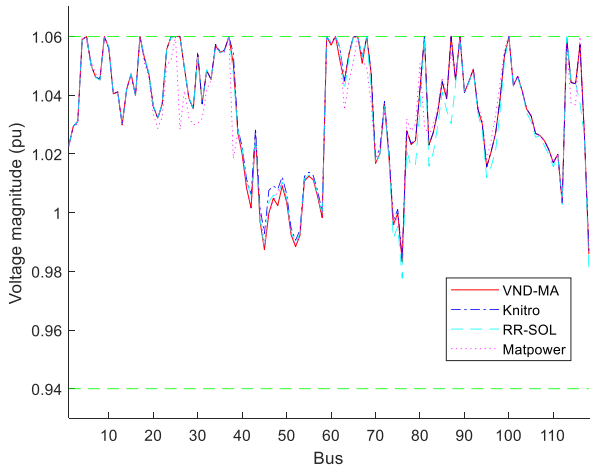

FIGURE 3. Voltage profile of the of the pglib_opf_case118_ieee system.

For example, the solutions obtained with Knitro and the proposed VND-MA have a total reactive shunt injection of 145.96 and 139.37 MVAr, respectively. This is because the shunt compensators at nodes 5 and 37 are disconnected. Finally, Matpower and the RR-SOL have a total reactive shunt injection of 86.43 and 81.99 MVAr, respectively.

For this system, the minimum and maximum voltage magnitude limits are 0.94 and 1.06, respectively, and all the obtained solutions are within these limits. Fig. 3 shows that the voltage profile of the solutions obtained with Knitro and the proposed VND-MA are quite similar in all the buses. On the other hand, notable differences can be observed in the voltage profile of the solutions obtained with the proposed RR-SOL and Matpower when compared with Knitro's solution.

B. TEST SYSTEMS

For all the test systems, Table 5 shows the most relevant results obtained solving the model (1)-(17) with the solver Knitro, the rounded strategy RR-SOL, Matpower, and the proposed VND-MA, including the value of the objective function, the CPU time, and the number of iterations of the VND-MA algorithm. In our experiments, the solutions found by the RR-SOL are feasible solutions. However, note that the RR-SOL strategy could find infeasible solutions for other power systems.

Table 6 shows the difference in generation costs and the respective percentage between RR-SOL/VND-MA, Knitro/VND-MA, and Matpower/VND-MA. The negative values in Table 6 indicate the test systems where Knitro and Matpower found better solutions than the VND-MA, while the positive values indicate where the proposed VND-MA found better solutions than the other approaches. Finally, a summary of the better results is presented in Table 7, where check (✓) indicates which approach has the better solution and circle (○) indicates an equal solution for the approaches

V. DISCUSSION

Comparing the rounded solution (RR-SOL) with the solution provided by the proposed VND-MA, the proposed methodology obtains better solutions for 88.23% of the systems tested and only two systems (pglib_opf_case14_ieee and pglib_opf_case30_ieee) where the algorithm was unable to improve the rounded solution. For large systems (pglib_opf_case3012wp_k and pglib_opf_case4661_sdet), the proposed VND-MA provides significantly better solutions with a reduction in the generation cost of 4.68% and 19.95% respectively. These results show that for small systems, the proposed algorithm to generate the initial solution finds high-quality solutions, however, a specialized optimization algorithm is necessary to solve medium- and large-scale systems.

For 47.06% of the systems tested, Knitro did not converge, i.e., the execution of the optimization solver was interrupted because it exceeded the established time limit (5 hours). Comparing Knitro with the proposed VND-MA, the proposed algorithm obtains better results for 58.82% of the systems tested. For systems until 118 buses the solver Knitro provides better solutions, however, note that the maximum profit is 0.0011% in the solution of the system pglib_opf_case89_pegase. On the other hand, for medium- and large-scale systems, starting from the pglib_opf_case200_tamu system to the pglib_opf_case3375wp_k system the proposed VND-MA provides better solutions than Knitro, besides, the CPU time is significantly less for all these systems. For cases where the solver Knitro was forced to stop the optimization process for exceeding the processing time, the proposed VND-MA provides better results, and the processing time has been reduced

TABLE 5. Fuel generation cost and processing time.

System	Knitro		RR-SOL		Matpower	VND-MA		
	Total fuel cost [$/h]	CPU time [s]	Total fuel cost [$/h]	CPU time [s]	Total fuel cost [$/h]	Total fuel cost [$/h]	CPU time [s]	Number of iterations
pglib_opf_case14_ieee	2177.29	0.08	2177.29	0.08	2178.08	2177.29	0.63	9
pglib_opf_case24_ieee_rts	63334.12	0.17	63334.31	0.08	63352.2	63334.12	0.59	8
pglib_opf_case30_ieee	8177.92	0.39	8178.19	0.08	8208.52	8178.18	0.78	12
pglib_opf_case39_epri	138390.06	2.89	138391.78	0.19	138415.56	138390.31	1.06	11
pglib_opf_case57_ieee	37550.48	10.41	37551.04	0.14	37589.34	37550.61	0.69	6
pglib_opf_case89_pegase	106489.34	16170.97	106620.83	0.42	107285.67	106490.56	11.33	46
pglib_opf_case118_ieee	97136.77	12.42	97142.58	0.28	97213.61	97137.27	4.03	22
pglib_opf_case200_tamu	27572.09	7820.84	27553.66	0.5	27557.57	27553.02	4.86	20
pglib_opf_case300_ieee	545908.8	18002.67	545564.68	0.47	565219.99	545555.89	2.94	6
pglib_opf_case500_tamu	72266.94	18025.62	72314.68	0.8	72578.3	72266.93	7.3	12
pglib_opf_case2000_tamu	1230189.56	18020.86	1227572.85	8.06	1228487.06	1226955.22	77.14	17
pglib_opf_case2383wp_k	1858267.5	18017.38	1858632.08	6.25	1868191.64	1858244.92	46.63	11
pglib_opf_case2746wp_k	1630283.75	18003.36	1631677.36	7.72	1631707.93	1630238.71	79.7	16
pglib_opf_case3012wp_k	2594182.32	18000.86	2721290.9	25.66	2600842.77	2593986.6	130.39	19
pglib_opf_case3120sp_k	2144516.04	18004.53	2144942.44	7.05	2147969.11	2144503.35	1321.81	12
pglib_opf_case3375wp_k	7427299.79	473.59	7430647.5	14.8	7438169.48	7427199.25	173.38	15
pglib_opf_case4661_sdet	2254217.61	18001.17	2815729.43	45.44	2251344.08	2254129.08	1860.25	44

TABLE 6. Difference in fuel generation costs.

System	RR-SOL / VND-MA		KNITRO / VND-MA		Matpower / VND-MA	
	Difference [$/h]	[%]	Difference [$/h]	[%]	Difference [$/h]	[%]
pglib_opf_case14_ieee	0	0	0	0	0.79	0.0363
pglib_opf_case24_ieee_rts	0.19	0.0003	0	0	18.08	0.0285
pglib_opf_case30_ieee	0	0	-0.26	-0.0032	30.34	0.3696
pglib_opf_case39_epri	1.47	0.0011	-0.25	-0.0002	25.25	0.0182
pglib_opf_case57_ieee	0.43	0.0011	-0.13	-0.0003	38.73	0.103
pglib_opf_case89_pegase	130.27	0.1222	-1.22	-0.0011	795.11	0.7411
pglib_opf_case118_ieee	5.31	0.0055	-0.5	-0.0005	76.34	0.0785
pglib_opf_case200_tamu	0.64	0.0023	19.07	0.0692	4.55	0.0165
pglib_opf_case300_ieee	8.79	0.0016	352.91	0.0646	19664.1	3.479
pglib_opf_case500_tamu	47.75	0.066	0.01	0	311.37	0.429
pglib_opf_case2000_tamu	617.63	0.0503	3234.34	0.2629	1531.84	0.1247
pglib_opf_case2383wp_k	387.16	0.0208	22.58	0.0012	9946.72	0.5324
pglib_opf_case2746wp_k	1438.65	0.0882	45.04	0.0028	1469.22	0.09
pglib_opf_case3012wp_k	127304.3	4.6781	195.72	0.0075	6856.17	0.2636
pglib_opf_case3120sp_k	439.09	0.0205	12.69	0.0006	3465.76	0.1614
pglib_opf_case3375wp_k	3448.25	0.0464	100.54	0.0014	10970.23	0.1475
pglib_opf_case4661_sdet	561600.35	19.9451	88.53	0.0039	-2785	-0.1237

TABLE 7. Best obtined results.

System	KNITRO	RR-SOL	VND-MA	Matpower
pglib_opf_case14_ieee	○	○	○	-
pglib_opf_case24_ieee_rts	○	-	○	-
pglib_opf_case30_ieee	✓	-	-	-
pglib_opf_case39_epri	✓	-	-	-
pglib_opf_case57_ieee	✓	-	-	-
pglib_opf_case89_pegase	✓	-	-	-
pglib_opf_case118_ieee	✓	-	-	-
pglib_opf_case200_tamu	-	-	✓	-
pglib_opf_case300_ieee	-	-	✓	-
pglib_opf_case500_tamu	-	-	✓	-
pglib_opf_case2000_tamu	-	-	✓	-
pglib_opf_case2383wp_k	-	-	✓	-
pglib_opf_case2746wp_k	-	-	✓	-
pglib_opf_case3012wp_k	-	-	✓	-
pglib_opf_case3120sp_k	-	-	✓	-
pglib_opf_case3375wp_k	-	-	✓	-
pglib_opf_case4661_sdet	-	-	-	✓

by an average of 97.31%. Note that, the solver Knitro reports a locally optimal solution for case pglib_opf_case3375wp_k in 439.09 seconds, however, the proposed VND-MA algorithm found an integer solution that is 12.69 $/h lower than the solution reported by Knitro.

As presented in Table 5, the minimum and maximum CPU time reported by the proposed VND-MA are 0.63s and 1860.25s, respectively. Note that, Knitro is faster than the proposed VND-MA only in the first three small systems, however, the VND-MA provides faster solutions for

the remaining medium- and large-scale systems. These results show that for medium- and large-scale systems, the proposed VND-MA presents a good trade-off between the total CPU time and the quality of the solutions. On the other hand, it is worth mentioning that the solution time highly depends on the efficiency of the optimization solver, then the number of iterations is not a suitable metric for the proposed VND-MA. It can be noted comparing the solution time for cases pglib_opf_case89_pegase and pglib_opf_case3120sp_k where the total CPU times were 11.33s and 1321.81s, respectively, however, the number of iterations were 46 and 12.

For illustrative purposes, Fig. 4 shows the convergence curve when using the proposed VND-MA to solve the pglib_opf_case3012wp_k system. This plot shows that the objective function value decreases rapidly over 9 iterations, then gradually decreases until it reaches the stopping criterion in iteration 19. Fig. 4 shows some iterations without improvements in the objective function value, this behavior indicates that the search strategy change to the next neighborhood structure. This is the expected behavior since the methodology is based on the VND algorithm.

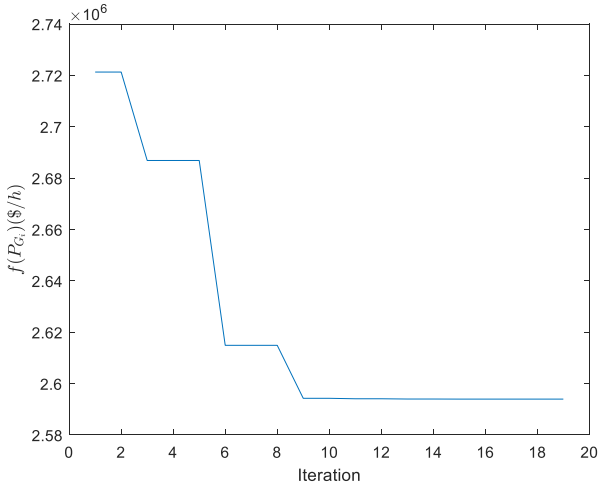

FIGURE 4. Convergence curve of the pglib_opf_case3012wp_k system.

Comparing the results provided by the proposed VND-MA and Matpower, the pglib_opf_case4661_sdet system is the only case in which Matpower obtains a solution that is 0.13% better than the solution found by the proposed VND-MA, however, the solution reported by Matpower does not consider the optimization of the integer variables in the resolution of OPF.

VI. CONCLUSION

This work presented a new matheuristic optimization methodology to solve the OPF problem considering a MINLP model. This is a new approach that combines the classic mathematical MINLP-OPF model with the philosophy of the VND heuristic algorithm.

Numerical experiments reveal that the commercial optimization solver Knitro provides high-quality solutions to this model for small- medium-scale power systems, however, its convergence process fails in the large-scale ones. On the other hand, the proposed VND-MA can solve even large-scale power systems in adequate computational time for solving the OPF problem for planning the operation giving high-quality solutions. In small-scale power systems, obtained results show similar solutions with both solution techniques, whereas, for medium- large-scale power systems, the advantage of the proposed VND-MA is evident since in all the cases it was possible to find better solutions.

In this paper, the polar formulation of the MINLP-FPO problem was considered, however, since the proposed neighborhood structures are based only on the integer variables of the problem, these can be used or adapted to solve other FPO formulations and approaches including convex or rectangular FPO formulations, single and multi-objective functions. Besides, similar strategies can be applied using other neighborhood algorithms including Tabu Search and all the variable neighborhood search algorithms.

REFERENCES

[1] H. W. Dommel and W. Tinney, "Optimal power flow solutions," *IEEE Trans. Power Appar. Syst.*, vol. PAS-87, no. 10, pp. 1866–1876, Oct. 1968.
[2] A. G. Bakirtzis, P. N. Biskas, C. E. Zoumas, and V. Petridis, "Optimal power flow by enhanced genetic algorithm," *IEEE Trans. Power Syst.*, vol. 17, no. 2, pp. 229–236, May 2002.
[3] H. R. E. H. Bouchekara, A. E. Chaib, and M. A. Abido, "Multiobjective optimal power flow using a fuzzy based grenade explosion method," *Energy Syst.*, vol. 7, no. 4, pp. 699–721, Nov. 2016.
[4] S. Frank, I. Steponavice, and S. Rebennack, "Optimal power flow: A bibliographic survey I," *Energy Syst.*, vol. 3, no. 3, pp. 221–258, Sep. 2012.
[5] S. Frank, I. Steponavice, and S. Rebennack, "Optimal power flow: A bibliographic survey II: Non-deterministic and hybrid methods," *Energy Syst.*, vol. 3, no. 3, pp. 259–289, Sep. 2012.
[6] D. K. Molzahn and I. A. Hiskens, "A survey of relaxations and approximations of the power flow equations," *Found. Trends Electric Energy Syst.*, vol. 4, nos. 1–2, pp. 1–221, 2019.
[7] F. Zohrizadeh, C. Josz, M. Jin, R. Madani, J. Lavaei, and S. Sojoudi, "A survey on conic relaxations of optimal power flow problem," *Eur. J. Oper. Res.*, vol. 287, no. 2, pp. 391–409, Dec. 2020.
[8] C. R. N. Estevam, M. J. Rider, E. Amorim, and J. R. S. Mantovani, "Reactive power dispatch and planning using a non-linear branch-and-bound algorithm," *IET Gener. Transm. Distrib.*, vol. 4, no. 8, pp. 963–973, Aug. 2010.
[9] I. Khan, V. Bhattacharjee, and M. Nasir, "Effect of the approximation of voltage angle difference on the OPF algorithms in the power network," *Energy Syst.*, vol. 11, no. 2, pp. 471–490, May 2020.
[10] G. L. Torres and V. H. Quintana, "An interior-point method for nonlinear optimal power flow using voltage rectangular coordinates," *IEEE Trans. Power Syst.*, vol. 13, no. 4, pp. 1211–1218, Nov. 1998.
[11] Z. Yang, H. Zhong, Q. Xia, A. Bose, and C. Kang, "Optimal power flow based on successive linear approximation of power flow equations," *IET Gener., Transmiss. Distrib.*, vol. 10, no. 14, pp. 3654–3662, Nov. 2016.
[12] R. A. Jabr, "Optimal power flow using an extended conic quadratic formulation," *IEEE Trans. Power Syst.*, vol. 23, no. 3, pp. 1000–1008, Aug. 2008.
[13] S. H. Low, "Convex relaxation of optimal power flow—Part I: Formulations and equivalence," *IEEE Trans. Control Netw. Syst.*, vol. 1, no. 1, pp. 15–27, Mar. 2014.
[14] X. Bai, H. Wei, K. Fujisawa, and Y. Wang, "Semidefinite programming for optimal power flow problems," *Int. J. Electr. Power Energy Syst.*, vol. 30, nos. 6–7, pp. 383–392, Jul. 2008.
[15] D. K. Molzahn and I. A. Hiskens, "Convex relaxations of optimal power flow problems: An illustrative example," *IEEE Trans. Circuits Syst. I, Reg. Papers*, vol. 63, no. 5, pp. 650–660, May 2016.

[16] D. K. Molzahn, J. T. Holzer, B. C. Lesieutre, and C. L. DeMarco, "Implementation of a large-scale optimal power flow solver based on semidefinite programming," *IEEE Trans. Power Syst.*, vol. 28, no. 4, pp. 3987–3998, Nov. 2013.
[17] T. Sousa, J. Soares, Z. A. Vale, H. Morais, and P. Faria, "Simulated annealing Metaheuristic to solve the optimal power flow," in *Proc. IEEE Power Energy Soc. Gen. Meeting*, Jul. 2011, pp. 1–8.
[18] C. A. Roa-Sepulveda and B. J. Pavez-Lazo, "A solution to the optimal power flow using simulated annealing," *Int. J. Electr. Power Energy Syst.*, vol. 25, no. 1, pp. 47–57, Jan. 2003.
[19] M. A. Abido, "Optimal power flow using tabu search algorithm," *Electr. Power Compon. Syst.*, vol. 30, no. 5, pp. 469–483, May 2002.
[20] M. S. Osman, M. A. Abo-Sinna, and A. A. Mousa, "A solution to the optimal power flow using genetic algorithm," *Appl. Math. Comput.*, vol. 155, no. 2, pp. 391–405, Aug. 2004.
[21] J. Yuryevich and K. P. Wong, "Evolutionary programming based optimal power flow algorithm," *IEEE Trans. Power Syst.*, vol. 14, no. 4, pp. 1245–1250, Nov. 1999.
[22] M. A. Abido, "Optimal power flow using particle swarm optimization," *Int. J. Elect. Power Energy Syst.*, vol. 24, no. 7, pp. 563–571, Oct. 2002.
[23] A. A. A. El Ela, M. A. Abido, and S. R. Spea, "Optimal power flow using differential evolution algorithm," *Electr. Power Syst. Res.*, vol. 80, no. 7, pp. 878–885, Jul. 2010.
[24] T. N. L. Anh, D. N. Vo, W. Ongsakul, P. Vasant, and T. Ganesan, "Cuckoo optimization algorithm for optimal power flow," in *Proc. 18th Asia Pacific Symp. Intell. Evol. Syst.*, 2015, pp. 479–493.
[25] M. Ghasemi, S. Ghavidel, M. Gitizadeh, and E. Akbari, "An improved teaching–learning-based optimization algorithm using Lévy mutation strategy for non-smooth optimal power flow," *Int. J. Electr. Power Energy Syst.*, vol. 65, pp. 375–384, Feb. 2015.
[26] H. R. E. H. Bouchekara, M. A. Abido, A. E. Chaib, and R. Mehasni, "Optimal power flow using the league championship algorithm: A case study of the Algerian power system," *Energy Convers. Manage.*, vol. 87, pp. 58–70, Nov. 2014.
[27] H. R. E. H. Bouchekara, "Optimal power flow using black-hole-based optimization approach," *Appl. Soft Comput.*, vol. 24, pp. 879–888, Nov. 2014.
[28] V. Yadav and S. P. Ghoshal, "Optimal power flow for IEEE 30 and 118-bus systems using monarch butterfly optimization," in *Proc. Technol. Smart-City Energy Secur. Power (ICSESP)*, Mar. 2018, pp. 1–6.
[29] S. Duman, U. Güvenç, Y. Sönmez, and N. Yörükeren, "Optimal power flow using gravitational search algorithm," *Energy Convers. Manage.*, vol. 59, pp. 86–95, Jul. 2012.
[30] A. K. Das, R. Majumdar, B. K. Panigrahi, and S. S. Reddy, "Optimal power flow for Indian 75 bus system using differential evolution," in *Swarm, Evolutionary, and Memetic Computing* (Lecture Notes in Computer Science), vol. 7076. Berlin, Germany: Springer, 2011, pp. 110–118, doi: 10.1007/978-3-642-27172-4_14.
[31] S. S. Reddy, P. R. Bijwe, and A. R. Abhyankar, "Faster evolutionary algorithm based optimal power flow using incremental variables," *Int. J. Electr. Power Energy Syst.*, vol. 54, pp. 198–210, Jan. 2014.
[32] S. S. Reddy and P. R. Bijwe, "Efficiency improvements in meta-heuristic algorithms to solve the optimal power flow problem," *Int. J. Electr. Power Energy Syst.*, vol. 82, pp. 288–302, Nov. 2016.
[33] T. Niknam, M. R. Narimani, and M. Jabbari, "Dynamic optimal power flow using hybrid particle swarm optimization and simulated annealing," *Int. Trans. Electr. Energy Syst.*, vol. 23, no. 7, pp. 975–1001, Oct. 2013.
[34] S. S. Reddy, "Multi-objective based adaptive immune algorithm for solving the economic and environmental dispatch problem," *Int. J. Appl. Eng. Res.*, vol. 12, no. 6, pp. 1043–1048, 2017.
[35] S. S. Reddy, "Multi-objective optimization considering cost, emission and loss objectives using PSO and fuzzy approach," *Int. J. Eng. Technol.*, vol. 7, no. 3, pp. 1552–1557, 2018.
[36] A. Y. Abdelaziz, E. S. Ali, and S. M. A. Elazim, "Combined economic and emission dispatch solution using flower pollination algorithm," *Int. J. Electr. Power Energy Syst.*, vol. 80, pp. 264–274, Sep. 2016.
[37] A.-A.-A. Mohamed, Y. S. Mohamed, A. A. M. El-Gaafary, and A. M. Hemeida, "Optimal power flow using moth swarm algorithm," *Electric Power Syst. Res.*, vol. 142, pp. 190–206, Jan. 2017.
[38] M. A. Taher, S. Kamel, F. Jurado, and M. Ebeed, "Modified grasshopper optimization framework for optimal power flow solution," *Electr. Eng.*, vol. 101, no. 1, pp. 121–148, Apr. 2019.
[39] A.-F. Attia, R. A. E. Sehiemy, and H. M. Hasanien, "Optimal power flow solution in power systems using a novel sine-cosine algorithm," *Int. J. Electr. Power Energy Syst.*, vol. 99, pp. 331–343, Jul. 2018.
[40] H. R. E. H. Bouchekara, A. E. Chaib, M. A. Abido, and R. A. El-Sehiemy, "Optimal power flow using an improved colliding bodies optimization algorithm," *Appl. Soft Comput.*, vol. 42, pp. 119–131, May 2016.
[41] T. T. Nguyen, "A high performance social spider optimization algorithm for optimal power flow solution with single objective optimization," *Energy*, vol. 171, pp. 218–240, Mar. 2019.
[42] S. S. Reddy, "Optimal power flow using hybrid differential evolution and harmony search algorithm," *Int. J. Mach. Learn. Cybern.*, vol. 10, no. 5, pp. 1077–1091, May 2019.
[43] M. Abdo, S. Kamel, M. Ebeed, J. Yu, and F. Jurado, "Solving non-smooth optimal power flow problems using a developed grey wolf optimizer," *Energies*, vol. 11, no. 7, p. 1692, Jun. 2018.
[44] D. Sun, B. Ashley, B. Brewer, A. Hughes, and W. Tinney, "Optimal power flow by Newton approach," *IEEE Trans. Power App. Syst.*, vols. PAS-103, no. 10, pp. 2864–2880, Oct. 1984.
[45] J. L. Carpentier, "'CRIC', A new active-reactive decoupling process in load flows, optimal power flows and system control," *IFAC Proc.*, vol. 20, no. 6, pp. 59–64, Aug. 1987.
[46] V. Maniezzo, T. Stützle, and S. Voß, Eds., *Matheuristics Hybridizing Metaheuristics and Mathematical Programming*, vol. 10. Boston, MA, USA: Springer, 2010.
[47] P. Hansen and N. Mladenovic, "Variable neighborhood search," in *Handbook Metaheuristics*. Boston, MA, USA: Springer, 2003, ch. 6, pp. 145–184.
[48] S. Babaeinejadsarookolaee, A. Birchfield, R. D. Christie, C. Coffrin, C. DeMarco, R. Diao, M. Ferris, S. Fliscounakis, S. Greene, R. Huang, and C. Josz, "The power grid library for benchmarking AC optimal power flow algorithms," Aug. 2019, *arXiv:1908.02788*. [Online]. Available: http://arxiv.org/abs/1908.02788
[49] S. Fliscounakis, P. Panciatici, F. Capitanescu, and L. Wehenkel, "Contingency ranking with respect to overloads in very large power systems taking into account uncertainty, preventive, and corrective actions," *IEEE Trans. Power Syst.*, vol. 28, no. 4, pp. 4909–4917, Nov. 2013.
[50] R. D. Zimmerman, C. E. Murillo-Sanchez, and R. J. Thomas, "MATPOWER: Steady-state operations, planning, and analysis tools for power systems research and education," *IEEE Trans. Power Syst.*, vol. 26, no. 1, pp. 12–19, Feb. 2011.

JUAN M. HOME-ORTIZ received the B.Sc. and M.Sc. degrees in electrical engineering from the Universidad Tecnológica de Pereira, Colombia, in 2011 and 2014, respectively, and the Ph.D. degree in electrical engineering from São Paulo State University (UNESP), Ilha Solteira, Brazil, in 2019.

He is currently a postdoctoral research with UNESP. His research interests include development of methodologies for the optimization, planning, and control of electrical power systems.

WMERSON CLARO DE OLIVEIRA received the B.Sc. degree in electrical engineering from the Universidade do Estado de Mato Grosso (UNEMAT), Brazil, in 2018, and the M.Sc. degree in electrical engineering from São Paulo State University (UNESP), Ilha Solteira, Brazil, in 2020.

His research interest includes development of methodologies for the optimization of electrical power systems.

JOSÉ ROBERTO SANCHES MANTOVANI (Member, IEEE) received the B.Sc. degree in electrical engineering from São Paulo State University (UNESP), Ilha Solteira, Brazil, in 1981, and the M.Sc. and Ph.D. degrees in electrical engineering from the University of Campinas, Campinas, Brazil, in 1987 and 1995, respectively.

He is currently a Professor with the Department of Electrical Engineering, UNESP. His research interests include development of methodologies for the optimization, planning, and control of electrical power systems, and applications of artificial intelligence in power systems.